arXiv:1701.05362v1 [quant-ph] 19 Jan 2017

The effect of dipole-dipole interaction on tripartite entanglement in different cavities

Salman Khan[1*] and Munsif Jan[2]

[1]*Department of Physics, COMSATS Institute of Information Technology, Park Road, Islamabad 45550, Pakistan. and*

[2]*Department of Physics, Quaid-i-Azam University Islamabad, 45320, Pakistan*

(Dated: July 28, 2015)

Abstract

The effect of dipole-dipole interaction, the initial relative phase and the coupling strength with the cavity on the dynamics of three two level atoms in the good and the bad cavity regime are investigated. It is found that the presence of strong dipole-dipole interaction not only ensures avoiding entanglement sudden death but also retains entanglement for long time. The choice of the phase in the initial state is crucial to the operational regime of the cavity. Under specific conditions, the entanglement can be frozen in time to its initial values through strong dipole-dipole interaction. This trait of tripartite entanglement may prove helpful in engineering multiparticle entanglement for the practical realization of quantum technology.

PACS numbers: 03.65.Ud; 03.67.Mn; 42.50.Dv

Keywords: Tripartite entanglement, Dipole coupling, decoherence, Cavity

*Electronic address: sksafi@comsats.edu.pk

I. INTRODUCTION

Entanglement has been recognized as the first candidate in the list of non-classical correlations and is considered as a vital resource for quantum information science [1, 2]. It has been widely investigated and a number of schemes have been presented for its detection, quantification, applications and generation [3–8]. However, the main problem in utilizing its benefit in quantum information processing is its survival during the processing of information. Any principle quantum system used for processing information interacts with environment whose effect on entanglement between the components of a composite system leads to a number of undesirable consequences, such as loss of entanglement and entanglement sudden death (ESD) [9]. On the other hand, study like [10] shows that under certain conditions the environment can generate or reproduce entanglement. Although initially pointed out theoretically, most of these phenomenon have now become laboratory facts [11, 12].

Most of the previous studies on the dynamics of entanglement in the presence of environment are limited to very simplified situations. For instance, the behavior of entanglement between two atoms under the assumption of equal coupling strengths between the atoms and the cavity mode is analyzed in Ref. [13, 14]. This is not a valid assumption while dealing with an optical cavity. This issue is tackled in [15], however, the effect of dipole-dipole interaction is ignored as in [16], which was later on addressed in [17]. These and other related studies [18, 19] focus on the behavior of bipartite entanglement of two level atoms. The dynamics of entanglement in two three level atoms and in three two level atoms has also been investigated [20, 21]. However, these studies also ignore the broad perspective and limit their findings to more simplified scenario.

In this paper, we investigate the dynamics of tripartite entanglement by considering more realistic situation. That is, we consider three two level atoms each influenced by its own individual structured reservoir initially in the vacuum state. Each atom is coupled to its reservoir through a different coupling strength. The atoms are also coupled to each other by dipole-dipole interaction with a coupling strength different for each pair. Comparison in the dynamics of entanglement for pure and mixed initial states is made. The influence of the relative quantum phase in the initial state on the dynamics of entanglement is demonstrated. We show that through the sole control of dipole-dipole interaction ESD can safely be avoided.

Moreover, it is shown that the loss of entanglement can not only be slow down in time but can also be frozen in time by properly tuning the parameters of the cavity. We expect that due to the relaxed conditions, the results of our model may easily be realized in the laboratory.

II. THEORETICAL MODEL

Consider three two-level atoms coupled to each other through dipole-dipole interaction where each atom is individually influenced by an independent zero-temperature bosonic reservoir. Under the rotating wave approximation, the total Hamiltonian of the composite system can be expressed as the sum of three independent terms in the following way

$$H = H_0 + H_{int} + H_{dd}, \tag{1}$$

where H_0 represents the sum of Hamiltonians of the isolated atoms plus environments, H_{int} is the atom-environment interaction Hamiltonian and H_{dd} represents the dipole-dipole interaction between the atoms. These can, respectively, be expressed as follows

$$H_0 = \omega_1\sigma_+^{(1)}\sigma_-^{(1)} + \omega_2\sigma_+^{(2)}\sigma_-^{(2)} + \omega_3\sigma_+^{(3)}\sigma_-^{(3)} + \sum_k \omega_k b_k^\dagger b_k, \tag{2}$$

$$H_{int} = (\alpha_1\sigma_+^{(1)} + \alpha_2\sigma_+^{(2)} + \alpha_3\sigma_+^{(3)})\sum_k g_k b_k + H.c, \tag{3}$$

$$\begin{aligned} H_{dd} = {} & K_1(\sigma_+^{(1)}\sigma_-^{(2)} + \sigma_-^{(1)}\sigma_+^{(2)}) + K_2(\sigma_+^{(2)}\sigma_-^{(3)} + \sigma_-^{(2)}\sigma_+^{(3)}) \\ & + K_3(\sigma_+^{(1)}\sigma_-^{(3)} + \sigma_-^{(1)}\sigma_+^{(3)}). \end{aligned} \tag{4}$$

In the preceding equations, $\sigma_\pm^{(j)}$ $(j = 1, 2, 3)$ represent the inversion operators and ω_j the transition frequency of the jth atom, $b_k^\dagger$ (b_k) represents the creation (annihilation) operator of the kth mode of the environments with eigenfrequency ω_k. The α_j's are dimensionless parameters and are measures of the coupling strength between the cavity and the corresponding atom. These parameters vary with the strength of the cavity mode and the relative position of the corresponding atom [16]. If $\vec{d_j}$ represents the dipole moment of an atom and $\vec{r}_{ij} = \vec{r}_i - \vec{r}_j$ $(i \neq j)$, $(i = 1, 2, 3)$ stands for the relative position, then the static constants K_j are given by [17]

$$K_j = r_{ji}^{-3}(\vec{d_j}\cdot\vec{d_j} - 3(\overrightarrow{d}_j\cdot\overrightarrow{r}_{ji})(\overrightarrow{r}_{ji}\cdot\overrightarrow{d}_j)/r_{ji}^2). \tag{5}$$

In Eq. (5) the indices take the values such that when $j = 1$, $i = 2$; $j = 2$, $i = 3$; and $j = 3$, $i = 1$.

For an initial state of the form

$$|\psi(0)\rangle = (a\,|100\rangle_{123} + b\,|010\rangle_{123} + c\,|001\rangle_{123}) \otimes \left|\overline{0}\right\rangle, \tag{6}$$

where $|0\rangle$, $|1\rangle$ are the ground and excited states of an atom, $|a|^2 + |b|^2 + |c|^2 = 1$ and $\left|\overline{0}\right\rangle = \bigotimes_k |0_k\rangle$ are the vacuum states of the environment with mode k. In order to investigate the role of relative quantum phase, we will later replace $b = be^{i\phi}$. Our investigations mainly deal with initial states correspond to $\phi = \{0, \pi\}$. The time evolution of the composite system can be written as

$$|\psi(t)\rangle = c_{11}(t)\,|100\rangle\,|0_k\rangle + c_{12}(t)\,|010\rangle\,|0_k\rangle + c_{13}(t)\,|001\rangle\,|0_k\rangle + \sum_k c_k(t)\,|000\rangle\,|1_k\rangle\,, \tag{7}$$

where $|1_k\rangle$ represent a single photon in the kth mode of the reservoir. For mathematical convenience, we consider that the transition frequency ω_j is same for the three atoms and we denote it by ω_o. The rate equations for the time evolved probability amplitudes can be obtained from the solution of Schrodinger equation which take the following form

$$i\dot{c}_{11}(t) = \alpha_1 \sum_k g_k c_k(t) e^{-i(\omega_k - \omega_0)t} + K_1 c_{12}(t) + K_3 c_{13}(t), \tag{8}$$

$$i\dot{c}_{12}(t) = \alpha_2 \sum_k g_k c_k(t) e^{-i(\omega_k - \omega_0)t} + K_2 c_{13}(t) + K_1 c_{11}(t), \tag{9}$$

$$i\dot{c}_{13}(t) = \alpha_3 \sum_k g_k c_k(t) e^{-i(\omega_k - \omega_0)t} + K_2 c_{12}(t) + K_3 c_{11}(t), \tag{10}$$

$$i\dot{c}_k(t) = g_k^* c_k(t) e^{i(\omega_k - \omega_0)t} (\alpha_1 c_{11}(t) + \alpha_2 c_{12}(t) + \alpha_3 c_{13}(t)), \tag{11}$$

By integrating Eq. (11) and substituting the result into the rest three rate equations leads to the following form of the probability amplitudes

$$\begin{aligned} \dot{c}_{11}(t) \;=\; & -\int_0^t dt_1 G(t - t_1)\alpha_1(\alpha_1 c_{11}(t_1) + \alpha_2 c_{12}(t_1) + \alpha_3 c_{13}(t_1)) \\ & -iK_1 c_{12}(t) - iK_3 c_{13}(t), \end{aligned} \tag{12}$$

$$\begin{aligned} \dot{c}_{12}(t) \;=\; & -\int_0^t dt_1 G(t - t_1)\alpha_2(\alpha_1 c_{11}(t_1) + \alpha_2 c_{12}(t_1) + \alpha_3 c_{13}(t_1)) \\ & -iK_2 c_{13}(t) - iK_1 c_{11}(t), \end{aligned} \tag{13}$$

$$\dot{c}_{13}(t) = -\int_0^t dt_1 G(t-t_1)\alpha_3(\alpha_1 c_{11}(t_1) + \alpha_2 c_{12}(t_1) + \alpha_3 c_{13}(t_1)) \\ -iK_2 c_{12}(t) - iK_3 c_{11}(t), \tag{14}$$

$$c(t) = \sqrt{1 - |c_{11}(t)|^2 - |c_{12}(t)|^2 - |c_{13}(t)|^2}, \tag{15}$$

where $G(t-t_1)$ is the correlation function. For the reservoir being electromagnetic field inside a lossy cavity, the spectral density $J(\omega_k)$ is Lorentzian in nature. Under resonant interaction between an atom and its reservoir, the spectral density can be expressed as follows

$$J(\omega_k) = \mid g_k \mid^2 = \frac{\Re^2 \lambda}{\pi[(\omega_k - \omega_0)^2 + \lambda^2]}, \tag{16}$$

where the weight factor $\Re$ depends on the vacuum Rabi frequency and λ stands for the width of the distribution. The relative weight of these parameters describes the nature of the coupling and hence the corresponding dynamics of the system. For $\lambda < 2\Re$, the coupling is strong and the dynamics are non-Markovian due to the existence of oscillatory reversible decay. On the other hand, the dynamics are Markovian and the coupling is weak when $\lambda > 2\Re$ [22] . In terms of the spectral density, the correlation function becomes

$$G\left(t-t_1\right) = \int_{-\infty}^{\infty} d\omega_k J\left(\omega_k\right) e^{-i(\omega_k - \omega_0)(t-t_1)}. \tag{17}$$

With the help of Fourier transform and the residue theorem, this can be reduced to $G(t-t_1) = \Re^2 e^{-\lambda(t-t_1)}$, with the inverse of λ being the reservoir correlation time.

Following the pseudomode approach [22, 23] and taking the Laplace transform, the solutions to the rate equations become

$$sc_{11}(s) = a - ir_1 Rb(s) - iK[c_{12}(s) + c_{13}(s)], \tag{18}$$

$$sc_{12}(s) = b - ir_2 Rb(s) - iK[c_{13}(s) + c_{11}(s)], \tag{19}$$

$$sc_{13}(s) = c - ir_3 Rb(s) - iK[c_{12}(s) + c_{11}(s)], \tag{20}$$

$$sb(s) - b(0) = -\lambda b(s) - iR[r_1 c_{11}(s) + r_2 c_{12}(s) + r_3 c_{13}(s)], \tag{21}$$

where the use of pseudomode amplitude

$$b(t) = -iR\int_0^t e^{-\lambda(t-t_1)} dt_1[r_1 c_{11}(t_1) + r_2 c_{12}(t_1) + r_3 c_{13}(t_1)], \tag{22}$$

is made. Also, in the preceding equations, we have introduced the vacuum Rabi frequency $R = \Re\alpha_T$ and the relative coupling strengths $r_j = \alpha_j(\alpha_T)^{-1}$ with $\alpha_T = \sqrt{\alpha_1^2 + \alpha_2^2 + \alpha_3^2}$

being the total coupling strength. To reduce the mathematical rigor and put the equations in more compact form, we have used a uniform static constant $K_j = K$. However, the effect of K_j's being different on the dynamics of entanglement will also be discussed while depicting it graphically.

The density matrix of the composite system can be constructed from the probability amplitudes by first applying the inverse Laplace transform to the preceding equations. Partial tracing over the environment space, leaves the following reduced density matrix for the system of three atoms

$$\begin{aligned}\rho_G \;=\; & (1-|c_{11}(t)|^2-|c_{12}(t)|^2-|c_{13}(t)|^2)\,|000\rangle\langle 000| + |c_{13}(t)|^2\,|001\rangle\langle 001| + \\ & |c_{12}(t)|^2\,|010\rangle\langle 010| + |c_{11}(t)|^2\,|100\rangle\langle 100| + (c_{12}(t)c_{13}^*(t)\,|010\rangle\langle 001| + \\ & c_{11}(t)c_{13}^*(t)\,|100\rangle\langle 001| + c_{11}(t)c_{12}^*(t)\,|100\rangle\langle 010| + H.C). \end{aligned} \tag{23}$$

The explicit form of the relations for the probability amplitudes are given in the Appendix.

We use tripartite negativity as quantifier for tripartite entanglement. For a tripartite system, it is defined in terms of three bipartite negativities. The three bipartite negativities are obtained by dividing the system in a cyclic manner into three arbitrarily chosen bipartitions. Mathematically, it is given as follows [24]

$$\mathcal{N}^{(3)}(\rho) = \sqrt[3]{\mathcal{N}_{1-23}\mathcal{N}_{2-13}\mathcal{N}_{3-12}}, \tag{24}$$

where $\mathcal{N}_{i-jk}$ $(k = 1, 2, 3)$ stands for the bipartite negativities of the three arbitrary bipartitions of the whole system. For each bipartition, it is given by $\mathcal{N}_{i-jk} = [\sum \lambda_\mu(\rho^{T_i}) - 1]/2$, with $\lambda_\mu(\rho^{T_i})$ as the eigenvalues of the partial transposed density matrix ρ^{T_i} of the composite system with respect to subsystem i [25, 26].

We focus our analysis of the dynamics of tripartite entanglement to the following maximally mixed Werner like states

$$\rho(t) = \frac{1-p}{8} I_{8\times 8} + p\rho_G, \tag{25}$$

where the parameter p stands for the purity of the state and $I_{8\times 8}$ is the identity matrix.

The compact relations for the three bipartite negativities become

$$\mathcal{N}_{1-23} = \frac{1}{4}\left[-2 + |1-p| + |\nu_{11}| + |\nu_{12}| + \left|\mu_1^+\right| + \left|\mu_1^-\right|\right]. \tag{26}$$

$$\mathcal{N}_{2-13} = \frac{1}{4}\left[-2 + |1-p| + |\nu_{21}| + |\nu_{22}| + \left|\mu_2^+\right| + \left|\mu_2^-\right|\right]. \tag{27}$$

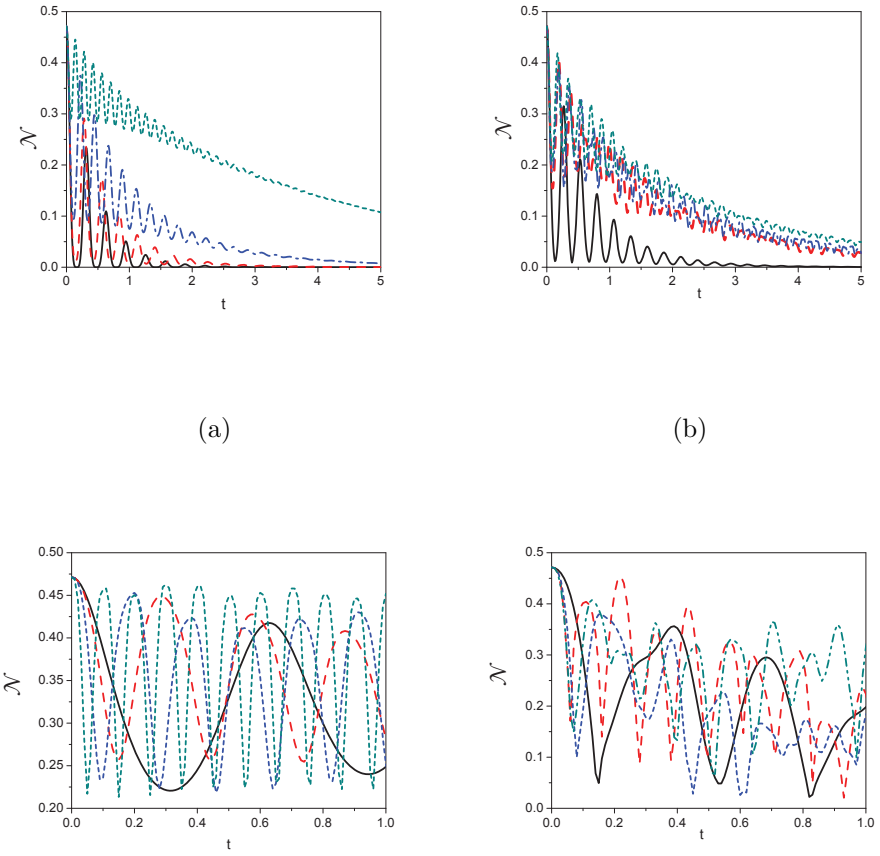

FIG. 1: (Color Online) The negativity both for uniform K (1st column) and non-uniform K (2nd column) is plotted against time t for $\phi = 0$ (1st row) and $\phi = \pi$ (2nd row) in the limit of good cavity. The other parameters in each figure are set to $a = b = c = \frac{1}{\sqrt{3}}$, $p = \lambda = 1$ and $r_1 = r_2 = r_3 = \frac{1}{\sqrt{3}}$ (1st column), $r_1 = \sqrt{\frac{2}{10}}$, $r_2 = \sqrt{\frac{3}{10}}$, $r_3 = \sqrt{\frac{5}{10}}$ (2nd column).

$$\mathcal{N}_{3-12} = \frac{1}{4}\left[-2 + |1-p| + |\nu_{31}| + |\nu_{32}| + \left|\mu_3^+\right| + \left|\mu_3^-\right|\right]. \tag{28}$$

where the detail relations for the new parameters are given in the Appendix. With everything in hand, we are in position to investigate the influence of different parameters on the tripartite entanglement of the system by using Eq. (24).

III. ANALYSIS AND DISCUSSION

In figure (1), we depict and compare the behavior of negativity against time for different set of values of K_j for two different initially pure states in the limit of good cavity ($R = 10$). The values of other parameters are given in the caption of the figure. The figures in the two rows, respectively, correspond to the two initial states different in phase with $\phi = 0$ and $\phi = \pi$. The first column represent the behavior of negativity for the two states with uniform static constant K for four difference values $K = 0, 5, 10, 20$. The second column represents the situation where each curve corresponds to a different set of values of K_j whose detail is given below.

It can be seen (figure($1a$)) that in the absence of dipole-dipole interaction ($K = 0$) the ESD and the revival of entanglement happen periodically with damped amplitude (solid black curve). This back and forth process will continue until the entanglement between the atoms is completely lost. On the other hand, the ESD can be completely avoid for $K \neq 0$. In this case, with the increase of oscillating frequency in the beginning a rapid decrease in the amplitude of oscillations happens that change it into a straight line in time with the increasing value of K (from bottom to top). This behavior of tripartite entanglement is opposite to the bipartite entanglement in which case the increasing value of K results in the rapid loss of entanglement [17]. However, for $\phi = \pi$ (figure($1c$)), the behavior of entanglement is completely different. In order to see an enlarge view of this different behavior (oscillations), we prefer to show plots by choosing a relatively short duration of time. In this case, no ESD occurs for any choice of the values of K and for every K the entanglement oscillates with damped amplitude about a mean value. For $K = 0$ (solid black curve), the oscillation's amplitude damps heavily about the mean and smoothen to a straight line as the time goes on ($t > 5$). For $K \neq 0$, the increasing value of K not only increases the frequency of oscillations but also increases its amplitude. Moreover, as the value of K increases, it considerably reduces the degree of damping per oscillation. The red-long dashed curve corresponds to $K = 5$, the blue-short dashed curve is for $K = 10$ and the cyan-dashed dotted curve is for $K = 20$. For non-uniform K, the ESD can be completely avoided for every set of values of K_j's, however, the entanglement loss may occur at delayed time. In the case of $\phi = 0$ (figure ($1b$)), although the amplitude of oscillation damps with time, however, it may exist for very long and may effect the periodicity of oscillations depending on the

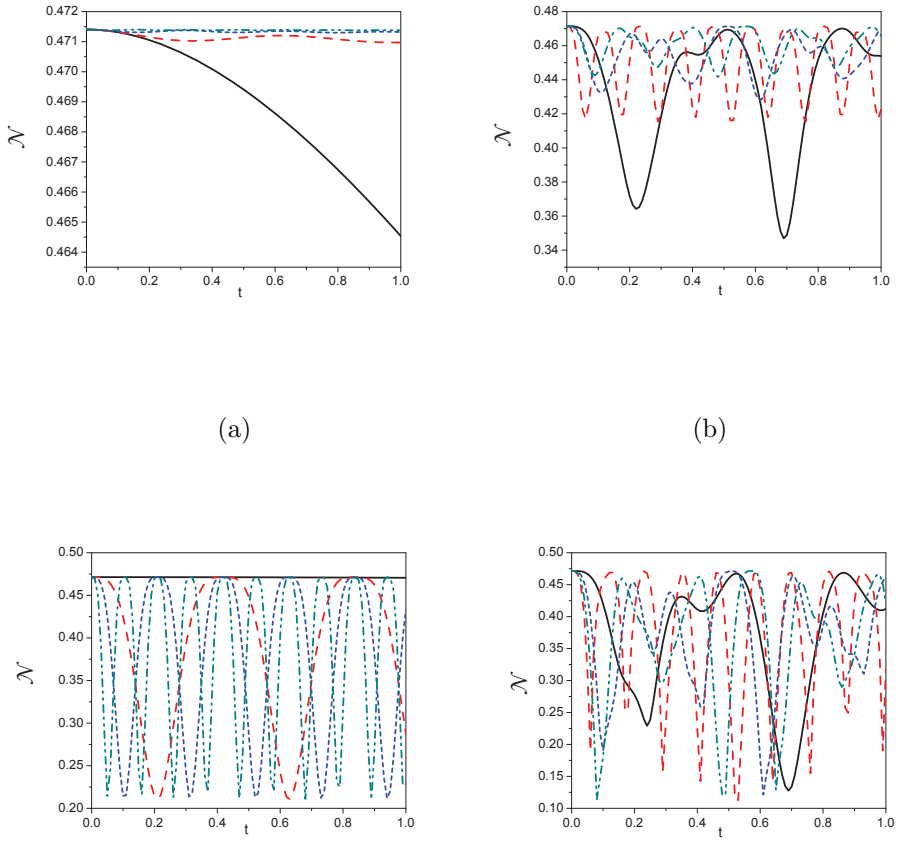

(a) (b)

(c) (d)

FIG. 2: (Color Online) The negativity both for uniform K (1st column) and non-uniform K (2nd column) is plotted against time t for $\phi = 0$ (1st row) and $\phi = \pi$ (2nd row) in the limit of bad cavity. The other parameters in each figure are set to $a = b = c = \frac{1}{\sqrt{3}}$, $p = \lambda = 1$ and $r_1 = r_2 = r_3 = \frac{1}{\sqrt{3}}$ (1st column), $r_1 = \sqrt{\frac{2}{10}}$, $r_2 = \sqrt{\frac{3}{10}}$, $r_3 = \sqrt{\frac{5}{10}}$ (2nd column).

choice of the set of values of K_j's. The set of values of K_j's for the curves are, black ($K_1 = 2$, $K_2 = 5$, $K_3 = 10$), blue ($K_1 = 10$, $K_2 = 15$, $K_3 = 20$), red ($K_1 = 2$, $K_2 = 18$, $K_3 = 20$) and cyan ($K_1 = 8$, $K_2 = 12$, $K_3 = 18$). Similarly, for $\phi = \pi$, the non-uniformity in K not only disturb the periodicity of oscillations but also affect the amplitude in different ways for every choice of the set of values of K_j's (figure ($1d$)). The choices for the set of values of K_j's are the same as in figure ($1b$).

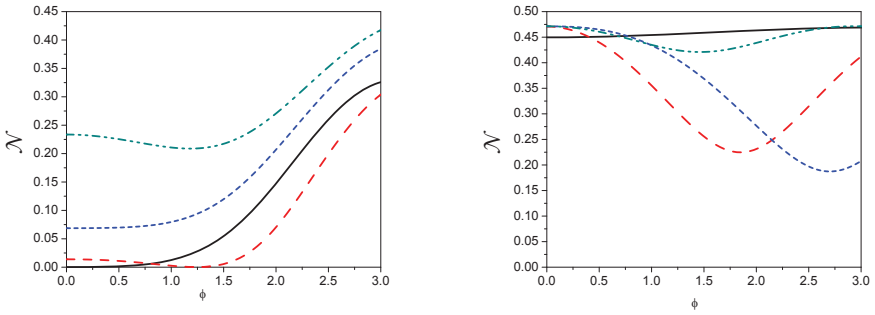

(a) (b)

FIG. 3: (Color Online) The negativity for uniform K is plotted against the relative phase ϕ. The other parameters in each figure are set to $a = b = c = \frac{1}{\sqrt{3}}$, $p = \lambda = 1$ and $r_1 = r_2 = r_3 = \frac{1}{\sqrt{3}}$.

In figure (2) we review figure (1) in the limit of bad cavity ($R = 0.1$) with other parameters remain unchanged. It can be seen from the comparison of the two figures that considerable changes in the behavior of entanglement in the presence of dipole-dipole interaction take place for the initial state with $\phi = 0$. The entanglement can be frozen to its initial value in the limit of strong dipole-dipole coupling ($K = 20$), the cyan-short dashed curve in figure (2a). For $\phi = \pi$, the entanglement is static for $K = 0$ and unaffected for the rest choices of the values of K (2b). In the case of non-uniform K_j's, except for the large difference in oscillating amplitudes, the behavior of entanglement for both initial states, qualitatively, becomes identical as shown in figures (2*b*, 2*d*). The amplitude of oscillations are considerably damped for the state with $\phi = 0$.

Figure (3) shows how will the entanglement dynamics be affected by the strength of dipole-dipole interaction for different choices of the initial relative phase in the limit of both good (figure (3*a*)) and bad (figure (3*b*)) cavities. The plots of both the figures are drawn with uniform K. The solid-black curve represents the $K = 0$ case, the red-dashed curve is for $K = 5$, the blue-dashed dotted and the cyan-dotted curve corresponds to $K = 10, 20$, respectively. In the limit of a good cavity ($R = 10$), the $\phi = \pi$ is always a good choice while on the contrary the $\phi = 0$ selection results in more entanglement irrespective of the value of K in the case of a bad cavity ($R = 0.1$). For a good cavity, beyond a certain limit, the

increasing value of K results in more entanglement for every choice of ϕ and get stronger at $\phi = \pi$. On the other hand, for a bad cavity the best choice is the absence of dipole-dipole interaction.

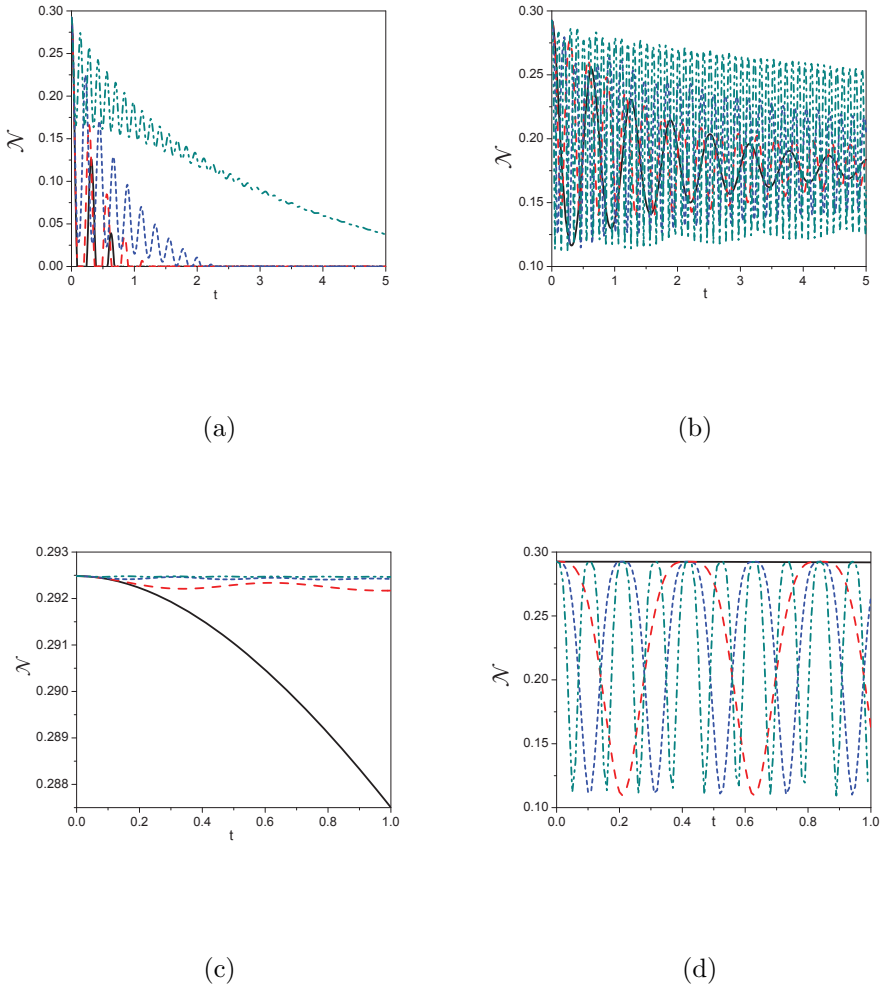

FIG. 4: (Color Online) The negativity in the limit of both good (1st row) and bad (2nd row) cavity for uniform K are plotted for two mixed initial states $\phi = 0$ (1st column) and $\phi = \pi$ (2nd column) with purity parameter $p = 0.7$. The values of other parameters are set to $a = b = c = \frac{1}{\sqrt{3}}$, $\lambda = 1$ and $r_1 = r_2 = r_3 = \frac{1}{\sqrt{3}}$.

The effect of purity parameter on the time evolution of the negativity is demonstrated in figure (4). The first row shows its behavior in a good cavity and the second row represents its behavior in the limit of a bad cavity. The two columns, respectively, correspond to the initial states with relative phases $\phi = 0$ and $\phi = \pi$. The values of all the parameters are

the same as in the first column of figure (1) except for $p = 0.7$. A comparison with the first column of figure (1) reveals that for initial state with $\phi = 0$, the overall behavior of negativity is qualitatively unchanged in the case of strong dipole-dipole interaction (the cyan-short dashed curve). However, for $K = 0$ (solid black curve) and for weak dipole-dipole interaction, the ESD occurs which is followed by its revival in a way that in each subsequent turn the amplitude is strongly damped which results shortly in the complete loss of entanglement. On the other hand, for the case of $\phi = \pi$ (figure (4*b*)), besides the initial overall damping the rest of the behavior, irrespective of the values of K, is qualitatively unchanged. Similarly, a comparison of the second row with the first column of figure (2) reveals that the qualitative behavior of pure and mixed initial states in the limit of bad cavity are identical.

IV. CONCLUSION

In this paper, we have investigated the influence of dipole-dipole interaction, initial relative quantum phase and the coupling strength of the system with the cavity on the behavior of entanglement between three two level atoms in the limit of both good and bad cavities. Comparison in the dynamics of tripartite entanglement between the choices of different initial states in both good and bad cavities under different sets of the controlling parameters is made. For a pure initial entangled state with zero relative phase in a good cavity, it is shown that the presence of strong dipole-dipole interaction not only avoid ESD but also enhances the retention of entanglement for long time both for uniform and non-uniform coupling of the system with the cavity. This behavior of tripartite entanglement is counterintuitive from the perspective of bipartite entanglement. Most importantly, it is shown that in the regime of bad cavity, the entanglement can be frozen to its initial value under strong dipole-dipole interaction. This behavior of tripartite entanglement is important for the practical realization of many suggested protocols for quantum information processing. Moreover, it is found that the choice of the phase in choosing initial state of the system is crucial to the characteristic of the cavity. We believe that our results may prove helpful to engineer multiparticle entanglement in laboratory for the accomplishment of many task in the foreseen quantum technology.

Acknowledgment

Munsif Jan is thankful to Razmi Fellowship for partially supporting this work under the Financial Assistance Program for Quaid-i-Azam University Islamabad, 45320, Pakistan.

V. APPENDIX

The explicit form of the probability amplitudes are given as follows

$$\begin{aligned} c_{11}(s) &= \frac{-be^{i\phi_1}(K_2K_3+iK_1s)-c(K_1K_2+iK_3s)+a(K_2^2+s^2)}{s^3+s(K_1^2+K_2^2+K_3^2)-2iK_1K_2K_3}+ \\ &\frac{ib(s)R(-r_1K_2^2+K_2(K_3r_2+K_1r_3)+is(K_1r_2+K_3r_3+ir_1s))}{s^3+s(K_1^2+K_2^2+K_3^2)-2iK_1K_2K_3}, \end{aligned} \tag{29}$$

$$\begin{aligned} c_{12}(s) &= \frac{-a(K_2K_3+iK_1s)-c(K_1K_3+iK_2s)+be^{i\phi_1}(K_3^2+s^2)}{s^3+s(K_1^2+K_2^2+K_3^2)-2iK_1K_2K_3}+ \\ &\frac{ib(s)R(K_3(K_2r_1-K_3r_2+K_1r_3)+is(K_1r_1+K_2r_3)-r_2s^2)}{s^3+s(K_1^2+K_2^2+K_3^2)-2iK_1K_2K_3}, \end{aligned} \tag{30}$$

$$\begin{aligned} c_{13}(s) &= \frac{-be^{i\phi_1}(K_1K_3+iK_2s)+a(K_1K_2+iK_3s)-c(K_1^2+s^2)}{s^3+s(K_1^2+K_2^2+K_3^2)-2iK_1K_2K_3}+ \\ &\frac{b(s)R(iK_1(-K_2r_1-K_3r_2+K_1r_3)+s(K_3r_1+K_2r_2)+ir_3s^2)}{s^3+s(K_1^2+K_2^2+K_3^2)-2iK_1K_2K_3}. \end{aligned} \tag{31}$$

The parameters in Eq. (26) are given as follows

$$\begin{aligned} \mu_1^{\pm} &= \nu_{13} \pm \sqrt{p(\nu_{14}-\nu_{15})}, \\ \nu_{11} &= \frac{1-p}{4}+2p\left|c_{11}(t)\right|^2, \\ \nu_{12} &= \frac{1-p}{4}+2p\left(1-\left|c_{11}(t)\right|^2-\left|c(t)\right|^2\right), \\ \nu_{13} &= \frac{1-p}{4}+p\left|c(t)\right|^2, \\ \nu_{14} &= \frac{1-p}{4}+4p\left|c_{11}(t)\right|^2\left(1-\left|c_{11}(t)\right|^2\right), \\ \nu_{15} &= \frac{1-p}{4}+p\left|c(t)\right|^2\left(4\left|c_{11}(t)\right|^2-\left|c(t)\right|^2\right). \end{aligned} \tag{32}$$

The parameters in Eq. (27) are given as follows

$$\begin{aligned}
\mu_2^{\pm} &= \nu_{13} \pm \sqrt{p(\nu_{23}-\nu_{24})}, \\
\nu_{21} &= \frac{1-p}{4} + 2p\left|c_{12}(t)\right|^2, \\
\nu_{22} &= \frac{1-p}{4} + 2p\left(1-\left|c_{12}(t)\right|^2-\left|c(t)\right|^2\right), \\
\nu_{23} &= \frac{1-p}{4} + 4p\left|c_{12}(t)\right|^2\left(1-\left|c_{12}(t)\right|^2\right), \\
\nu_{24} &= \frac{1-p}{4} + p\left|c(t)\right|^2\left(4\left|c_{12}(t)\right|^2-\left|c(t)\right|^2\right).
\end{aligned} \tag{33}$$

The parameters in Eq. (28) are given as follows

$$\begin{aligned}
\mu_3^{\pm} &= \nu_{13} \pm \sqrt{p(\nu_{33}-\nu_{34})}, \\
\nu_{31} &= \frac{1-p}{4} + 2p\left|c_{13}(t)\right|^2, \\
\nu_{32} &= \frac{1-p}{4} + 2p\left(1-\left|c_{13}(t)\right|^2-\left|c(t)\right|^2\right), \\
\nu_{33} &= \frac{1-p}{4} + 4p\left|c_{13}(t)\right|^2\left(1-\left|c_{12}(t)\right|^2\right), \\
\nu_{34} &= \frac{1-p}{4} + p\left|c(t)\right|^2\left(4\left|c_{13}(t)\right|^2-\left|c(t)\right|^2\right).
\end{aligned} \tag{34}$$

---

[1] M. Nielsen and I. Chuang, Quantum information and Computation Cambridge, Cambridge University (2000).

[2] R. Horodecki, P. Horodecki, M. Horodecki and K. Horodecki, Rev. Mod. Phys. 81 (2009) 865.

[3] C.H. Bennett, D.P. DiVincenzo, J.A. Smolin and W.K. Wootters, Phys. Rev. A. 54 (1996) 3824 .

[4] M. Horodecki, Quantum Inf. Comput. 1 (2001) 3.

[5] W.K. Wootters, Quantum Inf. Comput. 1 (2001) 27.

[6] Q.A. Turchette, C.S. Wood, B.E. King, C.J. Myatt, D. Leibfried, W.M. Itano, C. Monroe, D.J. Wineland, Phys. Rev. Lett. 81 (1998) 3631.

[7] X.G. Wang, Phys. Rev. A. 64 (2001) 012313.

[8] A. Aspect, P. Grangier, G. Roger, Phys. Rev. Lett. 47 (1981) 460.

[9] T. Yu, J.H. Eberly, Phys. Rev. Lett. 93 (2004) 140404.

[10] S. Khan, Math. Struct. in Comp. Science. 23 (2013) 1220.

[11] M.P. Almeida, F. de-Melo, M. Hor-Meyll, A. Salles, S.P. Walborn, P.H. Souto Ribeiro, L. Davidovich, Science. 316 (2007) 579.

[12] L. Aolita, R. Chares, D. Cavalcanti, A. Acín, L. Davidovich, Phys. Rev. Lett. 100 (2008) 080501.

[13] Z. Shi-Biao and G. Guang-Can, Phys. Rev. Lett. 85 (2000) 2392.

[14] S. Nicolosi, A. Napoli, A. Messina and F. Petruccione, Phys. Rev. A. 70 (2004) 022511.

[15] S. Natali and Z. Ficek, Phys. Rev. A. 75 (2007) 042307.

[16] S. Maniscalco, F. Francica, R. Zaffino, L. Rosa, N. Lo-Gullo and F. Plastina, Phys. Rev. Lett. 100 (2008) 090503.

[17] Y. Li, J. Zhou and H. Guo, Physical. Rev. A. 79 (2009) 012309.

[18] B. Wang, S. Xu, Y. Meng, Int. J. Theor. Phys. 52 (2013) 3604.

[19] J. Zhou, C. Wu, M. Zhu and H. Guo, J. Phys. B: At. Mol. Opt. Phys. 42 (2009) 215505.

[20] S. Zhan, Y. Li, K. Yeon, C. I. Um, J. Korean Phys. Soc. 45 (2004) 884.

[21] C.J. Shan, J.B. Liu, T. Chen, T.K. Liu, Y.X. Haung and H. Li, Chin. Phys. Lett. 27 (2010) 100301.

[22] B.J. Dalton, S.M. Barnett, B.M. Garraway, Phys. Rev. A. 64 (2001) 053801.

[23] B. M. Garraway, Phys. Rev. A. 55 (1997) 2290.

[24] F. Buscemi and P. Bordone, Phys. Rev. A. 87 (2013) 042310.

[25] A. Peres, Phys. Rev. Lett. 77 (1996) 1413.

[26] G. Vidal, R.F. Werner, Phys. Rev. A. 65 (2002) 032314.